 doi:10.20944/preprints202203.0319.v1

Unveiling the Mechanisms of High-temperature 1/2[111] Screw Dislocation Glide in Iron–Carbon Alloys

I. H. Katzarov[†‡], L. B. Drenchev[†]

† IMSET, Bulgarian Academy of Sciences,
67 Shipchenski prohod Str.,
Sofia 1574, Bulgaria
‡ Department of Physics, King's College London, Strand,
London WC2R 2LS, UK
email: ivaylo.katsarov@kcl.ac.uk

Abstract

We have developed a self-consistent model for predicting velocity of 1/2[111] screw dislocation in binary iron–carbon alloys gliding by a high-temperature Peierls mechanism. The methodology of modelling includes: (*i*) Kinetic Monte-Carlo (kMC) simulation of carbon segregation in dislocation core and determination the total carbon occupancy of the core binding sites; (*ii*) Determination of kink-pair formation enthalpy of a screw dislocation in iron—carbon alloy; (*iii*) KMC simulation of carbon drag and determination of maximal dislocation velocity at which the atmosphere of carbon atoms can follow a moving screw dislocation; (*iv*) Self consistent calculation of average velocity of screw dislocation in binary iron–carbon alloys gliding by a high-temperature kink-pair mechanism under constant strain rate. We conduct a quantitative analysis of the conditions of stress and temperature at which screw dislocation glide in iron–carbon alloy is accomplished by a high-temperature kink-pair mechanism. We estimate the dislocation's velocity at which screw dislocation brakes away from the carbon cloud and thermally-activated smooth dislocation propagation is interrupted by sporadic bursts controlled by athermal dislocation activity.

keywords: dislocations; diffusion; FeC alloy; Dynamic strain ageing

 doi:10.20944/preprints202203.0319.v1

1 Introduction

Steel plasticity is strongly influenced by interactions between solute atoms, such as carbon, and dislocations [1]. It is commonly accepted that the segregation of solute atoms in the surroundings of dislocations, forming clouds of impurities known as Cottrell atmospheres, is the underlying atomistic mechanism behind steel hardening [3, 4, 5]. The atmosphere is known to pin dislocations and render them less mobile. As more carbon atoms segregate, the atmosphere grows around the dislocations and hinders dislocation motion. Higher stresses are then required to unpin the dislocation from the solutes. The pinning/unpinning process results in a change of the mechanical properties of steels. The hardening of a material that is aged for a certain period of time after undergoing plastic deformation is commonly termed static strain aging. In contrast to static strain aging, which takes place during the specimen rest time, another strain aging phenomenon, called dynamic strain aging occurs during the plastic deformation of a specimen. It is associated with the diffusion of impurities to a mobile dislocation temporarily arrested at obstacles.

Recent measurements by Caillard [6] in binary iron–carbon alloys with carbon concentrations of 1, 16 and 230 atomic parts per million (appm) reveal that the dynamic interaction between mobile dislocations and solute carbon atoms results in dynamic strain aging effects in the temperature range of 100°C–300°C . Caillard found three regimes of behaviour: (*i*) the expected Peierls mechanism of kink pair formation and migration at low temperature; (*ii*) at intermediate temperatures carbon atoms become sufficiently mobile to move to the nearest dislocations and pin them. Dislocations start to move in bursts–no dislocation motion is observed upon straining during several minutes, until a source is unlocked and emits many dislocations. This results in the dynamic strain aging effect characterized by avalanches of rapid dislocation glide corresponding to the observed jerky and serrated flow. (*iii*) above about 200°C a new mechanism was discovered, namely viscous glide accomplished by a Peierls mechanism but with an activation energy almost twice that of the room temperature viscous flow. The transitions between these domains vary as a function of dislocation velocity, but so far a quantitative analysis has been lacking. One of the features of the problem has been a lack of detailed confirmation of observation with theory and modelling.

A dislocation drag mechanism, by which mobile dislocations can collect and transport carbon within their cores, takes place if the diffusion of carbon atoms and the motion of dislocations occur with rates in the same order of magnitude. It can be assumed that dislocations glide is accomplished by a high-temperature Peierls mechanism when carbon atoms in bcc-iron become

 doi:10.20944/preprints202203.0319.v1

mobile enough to follow gliding dislocations. To study drag of carbon atoms by dislocations requires simulation techniques that capture carbon diffusion events, trapping and escape from the core and the motion of dislocations simultaneously. Caillard [6] ascertained that dynamical strain aging is caused by the trapping of carbon by straight screw segments of 1/2[111] dislocations. For this reason we focus on the 1/2[111] screw dislocation in the present work. In [7] we have develop an atomistic kinetic Monte-Carlo (kMC) model describing carbon diffusion in the non-homogeneous stress field created by a 1/2[111] screw dislocation in bcc-iron, where the behaviour of individual atoms is explicitly taken into account. The kMC model employs information gathered from molecular statics simulations carried out in order to determine the activation energies required for carbon hops in the neighbourhood of the line defect [8]. The number of segregated carbon atoms forming a Cottrell atmosphere around a 1/2[111] screw dislocation, predicted by performing long time kMC simulations, has been validated against the carbon atmosphere visually identified by position-sensitive atom probe microscopy. kMC model allows us to study both the diffusing carbon residing in the dislocation core and carbon atoms which move through the interstitial sites in dislocation surroundings. We have employed the kMC model to simulate carbon diffusion in bcc–iron leading to the formation of Cottrell atmosphere. The kMC approach also offers an atomistic view of carbon drag mechanism by which mobile dislocations can collect and transport carbon within their cores. By setting dislocation to glide with constant velocity v_{dis} we can simulate the evolution of the carbon cloud arround the moving linear defect. This approach allows us to estimate the maximal dislocation velocity $v_{\max}(T, C)$ at which the atmosphere of carbon atoms can follow a moving screw dislocation. When dislocation velocity is higher than $v_{\max}$ dislocations gradually break away from the carbon clouds. Carbon atoms trapped in the core can follow the dislocation if it glides slowly and viscously via a Peierls mechanism, namely the process of kink pair creation followed by kink migration. However, we do not consider kink pair formation and migration explicitly in kMC model. We therefore turn now to the actual problem of predicting v_{dis} within the Peierls mechanism. Note that v_{dis} is then the dislocation velocity averaged over the multitude of the kink-pair creation and separation processes. The trapped C atoms strongly modify the kink pair formation enthalpy E_{kp}, which for a given resolved shear stress is a function of the the solute concentration and the rate at which impurities are distributed among trap sites [9]. At lower solute atom mobility the impurities remain behind in binding sites of higher potential energy as a dislocation segment moves between Peierls valleys, leading to a higher Peierls barrier and E_{kp}. The Peierls barrier becomes smaller as the rate at which solute atoms are dis-

 doi:10.20944/preprints202203.0319.v1

tributed among trap sites increases [9]. With increasing temperature, the number of solute atoms trapped in the core decreases, which also reduces the Peierls barrier [10]. Hence, as temperature increases E_{kp} decreases as a consequence of the decreasing Peierls barrier. It could be expected that a screw dislocation can glide via a high-temperature Peierls mechanism if: (a) the kink-pair formation energy barrier, E_{kp}, becomes smaller as the mobility of carbon atoms trapped in dislocation core increases at high temperature; (b) the carbon Cottrell atmosphere can follow the dislocation, that is, a dislocation's average velocity at given carbon concentration and temperature is lower than $v_{\max}$. The transitions to high-temperature viscous glide accomplished by a Peierls mechanism varies as a function of dislocation velocity. The problem of predicting v_{dis} within the Peierls mechanism is related to predicting kink-pair formation enthalpy E_{kp} at given carbon concentration and local shear stress τ. The purposes of the present work is conducting a quantitative analysis of the conditions of stress and temperature at which a transition may occur between carbon drag and breakaway and screw dislocation glide is accomplished by a high-temperature Peierls mechanism. Here, we present a self consistent model that is able to predict average velocity of screw dislocation in binary iron–carbon alloys gliding by a high-temperature kink-pair mechanism. The structure of the paper is as follows. Section 2 presents our methodology of modelling: In Sec. 2.1 we examine the effect of trapped carbon on motion of a straight dislocation between two adjacent Peierls valleys. Sec. 2.2 addresses the effect of carbon segregated in dislocation core on kink-pair formation. In Sec. 2.3 we present a self consistent model for determination of average velocity of screw dislocation in binary iron–carbon alloys gliding by a high-temperature kink-pair mechanism under constant strain rate. Sections 3 and 4 are our results and discussion sections. We conclude in Sec. 4.

2 Materials and Methods

2.1 Carbon effect on the dynamics of straight dislocation

Density functional theory (DFT) calculations have identified two core structures of the 1/2[111] screw dislocation, the so called easy core (EC), which is the stable, low energy configuration, and the hard core (HC) which is metastable [11, 12]. The HC is very close in configuration to the saddle point (SP) core [11, 12]. Tight-binding (TB) simulations of carbon interactions with the 1/2[111] screw dislocation found solute distribution to vary

Preprints (www.preprints.org) | NOT PEER-REVIEWED | Posted: 24 March 2022 doi:10.20944/preprints202203.0319.v1

significantly of the easy and hard cores [14]. The binding sites of carbon, and their strengths, were determined by the TB calculations of carbon-screw dislocation interactions. These were performed using the Fe-C TB model of Paxton and Elsässer [13]. The binding energies of carbon to both the hard and easy cores, with the resulting distribution of carbon can be seen in figure 1. These binding energies agree well with experiment and atomistic/elastic

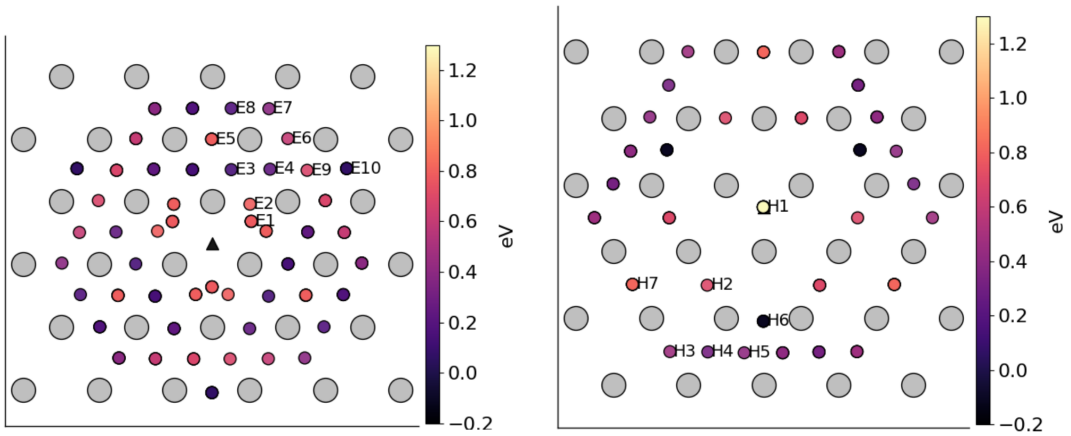

a) b)

Figure 1: The binding sites and binding energies of carbon segregated around: a) easy 1/2[111] screw dislocation core; b) hard 1/2[111] screw dislocation core.

calculations [12, 16]. In agreement with DFT the highest binding energy is found in the centre of the hard screw core [16]. As a dislocation moves from EC to HC to EC the traps sites ahead of the dislocation line transform into HC sites and finally the carbon occupies EC traps sites behind the dislocation line. These atomistic results provide data for determination of kink-pair formation energies as a function of stress and carbon concentration, C, using a line tension (LT) model of a dislocation [11]. A segment of a long dislocation lying in its Peierls valley has to migrate towards or into the next Peierls valley so as to make an incipient or complete kink pair. Within the LT model the dislocation is divided into segments of width b, the Burgers vector, along its length and a variable x_j is assigned to describe the deviation of the segment lying in the jth segment from the dislocations original position in the Peierls valleythe elastic center of the dislocation. The energy per unit length of dislocation is then described by the following line tension expression [11].

$$E = \sum_j E_j = \frac{1}{2} K \sum_j (x_j - x_{j+1})^2 + \sum_j E_P(x_j) + \sum_j \varepsilon_{1pq} \tau_{pr} b_r \xi_p x_j - \sum_k E_k^c(|x_j - x_C|) \tag{1}$$

 doi:10.20944/preprints202203.0319.v1

The first term describes the energy penalty for two segments which have different amounts of deviation from the original Peierls valley towards the next and K is the associated spring constant. The periodic Peierls energy landscape is described by an energy function, $E_P(x_j)$. The third term is the component perpendicular to line sense ξ of the Peach-Kohler force arising from a local stress τ times the displacement of the jth segment. The final term expresses the energy associated with a carbon atoms that are trapped at the binding sites in the dislocation core at a distance $|x_j - x_C|$ from core, in which x_C is the position of the kth carbon atom relative to the elastic centre. Here $0 < x < h$, where h is the period of the Peierls potential on the (110) plane. This term varies when a dislocation segment propagates between two adjacent Peierls as a result of the variation of the binding energies $E_k^c(x)$ and carbon redistribution between trap sites. We parameterise $E_k^c(x)$ by fitting and interpolation of tigth-binding data [14]. We define

$$\chi_t = \sum_i \chi_i = const \tag{2}$$

as the total carbon occupancy of the core sites and we will assume throughout that this is constant, that is, carbon will redistribute dynamically between trap sites during glide but overall the dislocation will not absorb or reject carbon. We also only allow C to redistribute among traps within a plane perpendicular to the dislocation line, in view of the slower carbon pipe diffusivity [7]. We define the equilibrium occupation probability, χ_i^e of trap site i as [15],

$$\chi_i^e(x) = \frac{\chi_i e^{-E_i^c(x)/kT}}{\sum_j \chi_j e^{-E_j^c(x)/kT}} \tag{3}$$

Once that is done, then in association with the line tension model (1) we have a complete description of the energetics of the dislocation as a function of x and the total occupancy, χ_t , for the moment only in two limiting cases: (a) equilibrium, slow glide in which traps are occupied according to (3), and (b) fast glide, in which all hydrogen atoms are fixed in the traps they occupy in the initial state before glide. Fig. 2 shows potential energy profiles in both limiting cases for carbon concentration in the bulk C=250 appm. In the equilibrium limit the effect of trapped carbon is strong enough so that for carbon concentration in the bulk, C=250 appm, the saddle point core is lower in energy than the easy core and their roles are reversed. This is because the total energy gained by carbon in deeper traps overwhelms the penalty in core energy. This result agrees well with DFT simulations by Ventelon [16]. When a carbon is placed in the vicinity of a relaxed easy dislocation core a spontaneous reconstruction of the dislocation core occurres: from

Preprints (www.preprints.org) | NOT PEER-REVIEWED | Posted: 24 March 2022 doi:10.20944/preprints202203.0319.v1

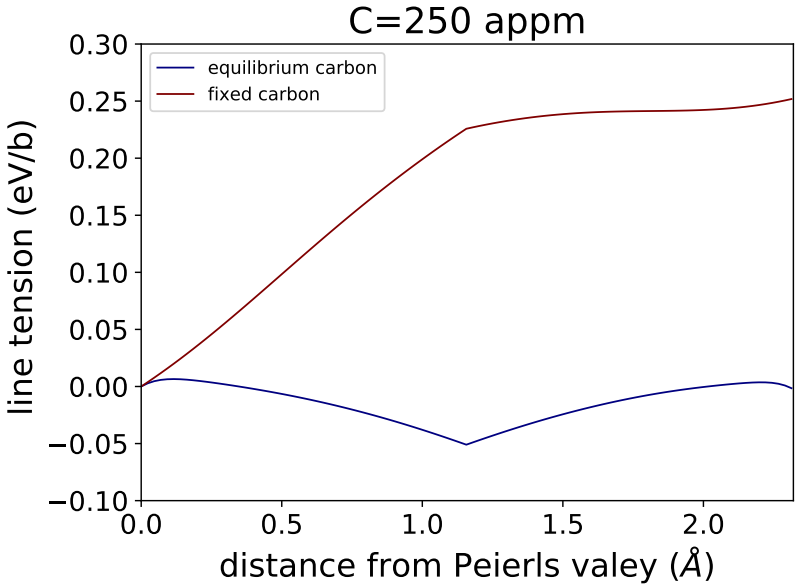

Figure 2: Potential energy of a straight 1/2[111] screw dislocation.

easy to hard. In the limit of rapid glide the carbon atoms are kept fixed during the movement of a dislocation between Peierls valleys. Then as the dislocation moves carbon remains behind in sites of higher potential energy. Hence, the Peierls barrier increases and the initial and final positions of the dislocation line have not the same energy. The actual potential energy profile will be controlled by the uniform dislocation velocity, v. Therefore we seek a theory that will predict the profile as a function of v. We may assume that the difference between the probability of occupancy of trap i, $\chi_i(x)$, and its equilibrium value (3), $\chi_i^e(x)$ is the driving force for carbon redistribution between trap sites. For any of the binding sites we find the following continuity equation,

$$\frac{\partial \chi_i(x,v)}{\partial t} = v\frac{\partial \chi_i(x,v)}{\partial x} = -\sum_{i\neq j}\left(\chi_i(x,v) - \chi_i^e(x)\right)R \tag{4}$$

where $R = fexp(-E_i(x)/kT)\left(\chi_j^e(x) - \chi_j(x,v)\right)$ if $(\chi_i > \chi_i^e)$ and $(\chi_i < \chi_i^e)$; $R = fexp(-E_j(x)/kT)\left(\chi_j(x,v) - \chi_j^e(x)\right)$ if $(\chi_i < \chi_i^e)$ and $(\chi_i > \chi_i^e)$; f is an attempt frequency for carbon to escape from the ith trap. By solving (4), subject to the condition (2) that the total carbon occupancy remains constant, we may determine the potential energy of the dislocation as a function of position between two Peierls valleys at velocity v.

Preprints (www.preprints.org) | NOT PEER-REVIEWED | Posted: 24 March 2022 doi:10.20944/preprints202203.0319.v1

2.2 Kink pair formation enthalpy

The thermal fluctuations produce random events in which a small section of screw dislocation deviates towards a neighbouring Peierls valley. Mostly this produces an incipient kink pair which annihilates due to elastic attraction of the kinks. The formation of a stable kink pair is a result of numerous acts of kink-pair nucleation, annihilation, and increasing distance between kinks under the action of the applied shear stress. We do not consider all these processes explicitly in our simulations. Trapped carbon strongly modifies the kink-pair formation energy, E_{kp}, and the distribution of carbon in traps will depend on how fast the dislocation is moving. Hence E_{kp} is a function of v_{dis} since it depends on the rate at which carbon is distributed among trap sites as the dislocation glides. For a given resolved shear stress, τ, and an assumed average velocity, v_{dis} , using the LT model the energy, $E_j(C, x, v_{dis})$, of a dislocation segment, Eq. (1), of length b and at a distance x from the initial Peierls valley, can be calculated. Then using the nudged elastic band (NEB) method [17], we may calculate the kink pair formation enthalpy, $E_{kp}(C, \tau, v_{dis})$ [10, 11]. However E_{kp} is a function of v_{dis} while v_{dis} is a function of E_{kp}. To find a self consistent solution, we assume that the average speed is constant, and

$$v_{dis}(E_{kp}) = \frac{h}{t_r} \tag{5}$$

allowing us to define an average relaxation time for kink-pair formation,

$$t_r = f_{kp}^{-1} e^{E_{kp}(C,\tau,v)/kT} \tag{6}$$

where f_{kp} is an attempt frequency. The frequency prefactor f_{kp} has been determined by comparing the velocity of a pure screw segment in bcc-Fe calculated from kMC model of 1/2[111] screw dislocation with the experimentally estimated velocity [10]. We find $f_{kp} = 2.31 \times 10^9\ s^1$. In order to solve (5) and (6), and to determine E_{kp} at given C and τ, we proceed with the following iterative process.

1. Assume an initial E_{kp}.
2. Calculate the corresponding v_{dis} using (5) and (6).
3. Determine the distribution of hydrogen from the continuity equation (4), subject to (2); and calculate the segment energy, $E_j(C, x, v_{dis})$ from the line tension model.
4. Calculate E_{kp} using the NEB and go to step 2.

This process is iterated until E_{kp} calculated in step 4 is no longer changing to within some tolerance.

Preprints (www.preprints.org) | NOT PEER-REVIEWED | Posted: 24 March 2022 doi:10.20944/preprints202203.0319.v1

2.3 Self-consistent calculation of dislocation velocity in binary iron–carbon alloys

The steady motion of screw dislocations is typical of the kink-pair mechanism, for which the velocity can be expressed as

$$v_{dis} = f_{kp}\frac{hL}{w}e^{-E_{kp}(\tau,C)/kT} \tag{7}$$

where w is the critical width of a stable kink pair and L is dislocation length. Molecular dynamics simulations have identified the critical width of the 1/2 [111] screw dislocation as $w \approx 30b$ [18]. If E_{kp} is small then kink pair formation is easy on all three [110] glide planes, and this leads to increased likelihood of kink pair collisions resulting in the formation of jogs [9, 10]. Eq. (7) does not take into account the effects of jog formation and self pinning on the dislocation mobility. In order to emulate experimental tests, which are performed under constant strain rate, $\dot{\varepsilon}_0$, and temperature, T, we carry out strain rate-controlled simulations. The instantaneous shear stress resulting from a given shear strain rate is obtained as:

$$\tau(t) = 2\mu[t\dot{\varepsilon}_0 - \varepsilon_p(t)] \tag{8}$$

where μ is the shear modulus, and ε_p is the total accumulated plastic strain

$$\varepsilon_p(t^{n+1}) = \varepsilon_p(t^n) + \delta\varepsilon_p(t^{n+1}) \tag{9}$$

t is the total simulation time and δt^{n+1} is the current time step. For its part, the plastic strain update is obtained from the dislocation velocities calculated at each stress using Orowans equation, as:

$$\delta\varepsilon_p(t^{n+1}) = \rho_d b v_{dis}(\tau)\delta t^{n+1} \tag{10}$$

where $v_{dis}(\tau)$ is the dislocation velocity, which depends on the resolved shear stress τ and carbon atoms trapped in the dislocation core; ρ_d is dislocation density. In order to determine self-consistently the velocity of screw dislocation in binary iron–carbon alloys gliding by a high-temperature Peierls mechanism, we proceed with the following iterative process.

1. Calculate the v_{dis} at initial shear stress τ using (7) and determined $E_{kp}(\tau, C)$.
2. From the dislocation velocity calculated at stress τ, we calculate the total accumulated plastic strain from (9) and (10).
3. The instantaneous shear stress τ resulting from the a calculated accumulated plastic strain is obtained from (8).

Preprints (www.preprints.org) | NOT PEER-REVIEWED | Posted: 24 March 2022 doi:10.20944/preprints202203.0319.v1

4. Go to step 1

If dislocation brakes away from the carbon cloud thermally-activated dislocation movement is replaced by athermal screw dislocation burst limited by phonon drag. In this case velocity v_{dis} is proportional to the driving force experienced by the dislocation

$$v_{dis} = \tau \frac{b}{B} \tag{11}$$

where B is the phonon drag coefficient. In the present work we use the temperature dependent value of the drag coefficient for kink motion $B = (2.7 + 0.008T) \times 10^5$ Pa s, determined by MD simulations [19].

3 Results

The kMC treatment of carbon Cottrell atmosphere formation presented in this work considers a portion of the atmosphere contained inside a fixed volume parallelepipedal region $10 \times 10 \times 10$ nm^3, the rectangular cross section of which (10×10 nm^2) corresponds approximately to the core region of the atom probe experiments. In the present study the surroundings of the

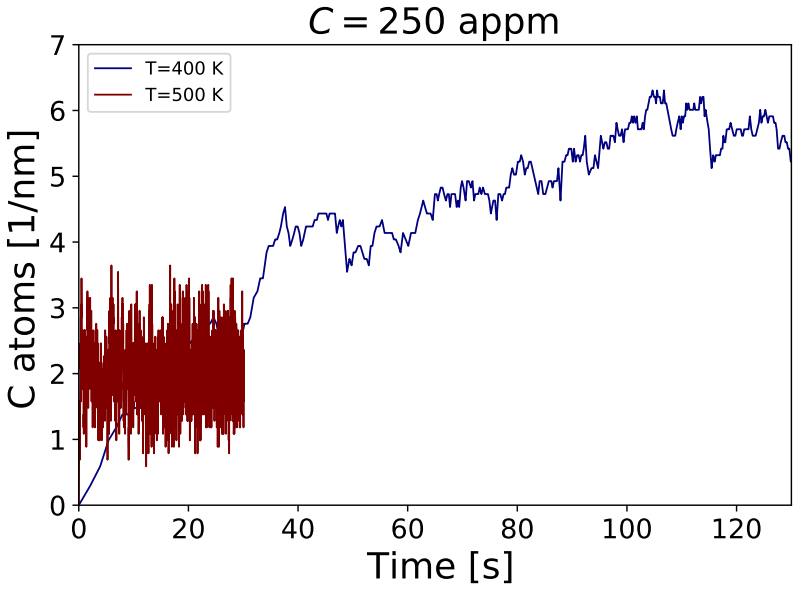

Figure 3: The number of carbon atoms per 1nm trapped in the dislocation core at two different temperatures.

dislocation core (region with radius $R \approx 0.6$ nm in the direct neighbourhood

Preprints (www.preprints.org) | NOT PEER-REVIEWED | Posted: 24 March 2022 doi:10.20944/preprints202203.0319.v1

of the dislocation centre [8]) are connected to an infinite carbon reservoir, such that no carbon depletion occurs in the matrix due to segregation [**?**]. The evolution of the number of carbon atoms segregated to form an atmosphere around a 1/2[111] screw dislocation at background carbon concentration 250 appm simulated by our kMC model is shown in Fig. 3. The kMC calculations

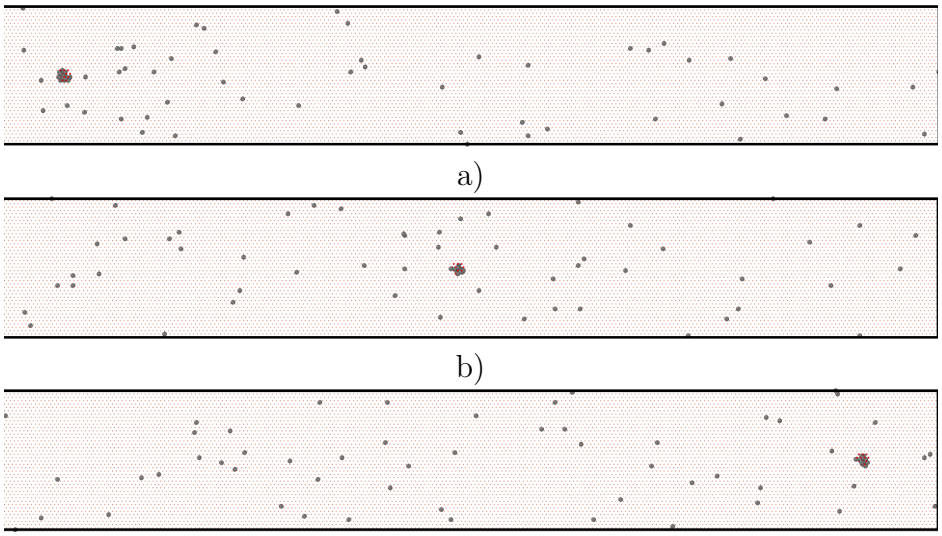

Figure 4: The motion of a screw dislocation dragging carbon ilustrated by a series of snapshots. KMC simulations are carried out at dislocation velocity $v_{dis} = 0.1$ nm/s and temperature 400 K

allow us to predict the rate of formation and strength of carbon atmospheres. The simulations show that at $T = 400$K an equilibrium carbon Cottrell atmosphere is formed after 100 seconds. At 500K the equilibrium carbon Cottrell atmosphere around a screw dislocation is formed even faster–0.3 sec for 250 appm. At equilibrium the average number of carbon atoms trapped in the screw dislocation core is around 5 C/nm at 400 K and 2.3 C/nm at 500 K. From these kMC simulations we determine the total carbon occupancy of the core binding sites χ_t.

The kMC treatment of the carbon drag mechanism presented in this section considers the evolution of the carbon cloud dragged by a mobile straight screw dislocation inside a fixed volume parallelepipedal region $60 \times 10 \times 10$ nm^3. At the starting time $t = 0$, the carbon atoms segregated to form an atmosphere around the 1/2[111] screw dislocation are at equilibrium with the background carbon concentration. We employ the kMC model to simulate the redistribution of carbon atoms when dislocation migrates in the (110) glide plane with constant velocity v_{dis} (Fig. 4). The number of carbon

Preprints (www.preprints.org) | NOT PEER-REVIEWED | Posted: 24 March 2022 doi:10.20944/preprints202203.0319.v1

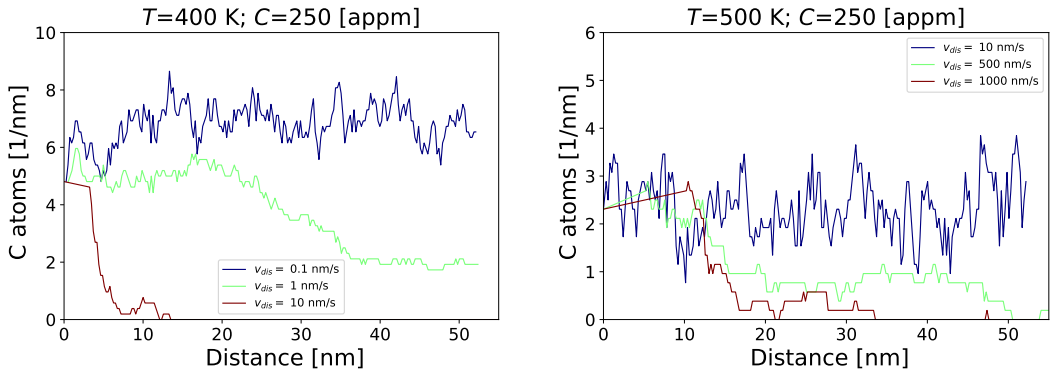

a) b)

Figure 5: The evolution of the number of carbon atoms per 1 nm trapped in the core of a moving straight dislocation as a function of the travel distance.

atoms effectively dragged by the dislocation as a function of the dislocation travel distance is shown in Fig. 5 for different dislocation velocities and temperatures of 400 K and 500 K. From the above simulations we evaluate the maximal dislocation velocity $v_{\max}$ at which the atmosphere of carbon atoms can follow a moving screw dislocation (Fig.6).

Figure 7 shows the results of the self-consistent iterative procedure for calculation of kink-pair formation enthalpy E_{kp} proposed in Sec. 2.2. We may interpret Fig. 7 in the following way. At high stress, E_{kp} is uniformly smaller because the applied stress acts to drive a dislocation into the next Peierls valley and this dominates the process of glide. At low stress we observe a large E_{kp} the largest being that of zero stress. As temperature increases, E_{kp} decreases as a consequence of the decreasing Peierls barrier due to enhanced carbon mobility and lower C occupancy in the core. After determination of E_{kp} as a function of τ and C, we apply the self-consistent procedure described in Sec. 2.3 to determine the evolution of 1/2[111] scew dislocation velocity during a strain rate-controlled simulation of dislocation motion in binary iron–carbon alloys. Dislocation density in our simulations is $\rho_d = 10^{13}\ m^{-2}$. This value of ρ_d also sets the dislocation line length to a magnitude of approximately $L = (\rho_d)^{-1/2}$, which for $\rho_d = 10^{13}\ m^{-2}$, gives $L = 1280b$. The simulations are performed under constant strain rate, $\varepsilon_0 = 10\ s^{-1}$. Evolution of the velocity and stress with time during a strain rate-controlled simulation of dislocation motion at T=400 K and T=500 K are shown respectively in Fig. 8 and Fig.9.

Preprints (www.preprints.org) | NOT PEER-REVIEWED | Posted: 24 March 2022 doi:10.20944/preprints202203.0319.v1

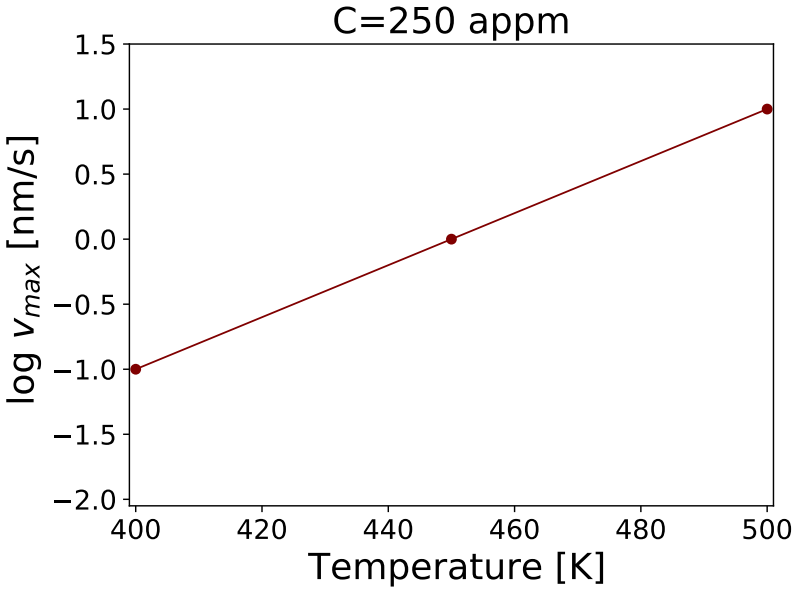

Figure 6: The maximal dislocation velocity $v_{\max}$ at which the atmosphere of carbon atoms can follow a moving screw dislocation at different temperatures.

4 Discussion

At 400 K carbon atoms become sufficiently mobile to move to the nearest dislocations and hinder dislocation motion. The trapped solute atoms remain behind in binding sites of higher potential energy as a dislocation segment moves, leading to a higher Peierls barrier and kink-pair formation energy E_{kp} (Fig.7). Higher stresses are then required to increase kink-pair formation rate and dislocation velocity. The carbon atoms have sufficient time to follow the dislocation at lower dislocation velocities (Fig 5a). kMC simulations reveal that at 400 K and background carbon concentration of 250 appm maximal dislocation velocity $v_{\max}$ at which the atmosphere of carbon atoms can follow a moving screw dislocation is 0.1 nm/s. The accumulated plastic strain induced by dislocations gliding at low velocities $v_{dis} < v_{max}$ can not relief efficiently the shear stress resulting from the constant shear strain rate (Fig. 8b). The rising shear stress increases the velocity of dislocations gliding by kink-pair mechanism. When v_{dis} exceeds v_{max} dislocations break away from the carbon clouds and start to move athermally and rapidly sliding above the Peierls barrier (Fig. 8a). In this case we calculate dislocation velocity using equation (11). The abrupt increase of the dislocation velocity reliefs the stress which results in decreasing v_d bellow v_{max}. After restoration of kink-pair glide dislocation velocity gradually increases above v_{max} leading to repeated

Preprints (www.preprints.org) | NOT PEER-REVIEWED | Posted: 24 March 2022 doi:10.20944/preprints202203.0319.v1

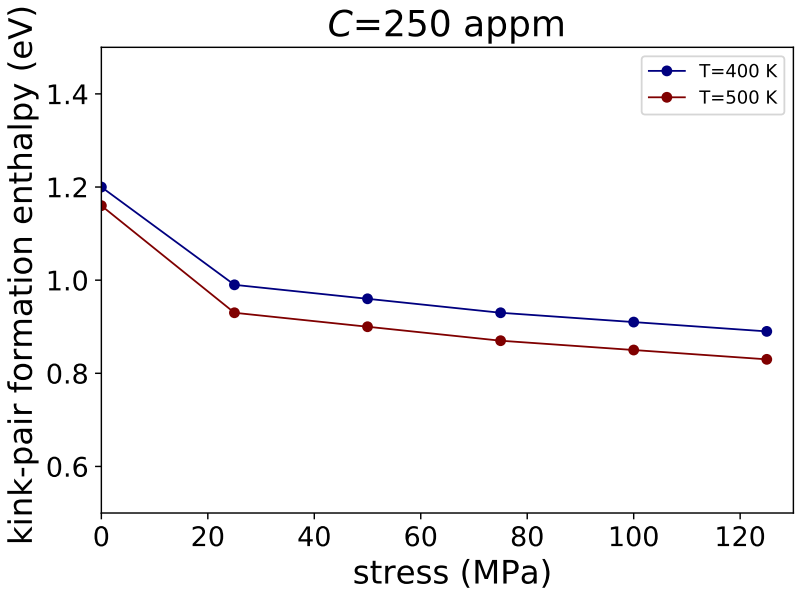

Figure 7: Kink pair formation enthalpy, E_{kp}, as a function of resolved shear stress, calculated by iterative solution of equations (5) and (6).

bursts of rapid dislocation glide. The studied thermally-activated smooth dislocation propagation is interrupted by abrupt sporadic bursts controlled by athermal screw dislocation activity.

At higher temperatures the number of carbon atoms trapped in the core decreases, which reduces the barrier between two adjacent Peierls valleys. The Peierls barrier is additionally reduced as the rate at which carbon atoms are distributed among trap sites increases. Hence, as temperature increases kink-pair formation enthalpy E_{kp} decreases as a consequence of the decreasing Peierls barrier (Fig.7). At higher temperatures carbon has a sufficiently high mobility to keep up with faster dislocations (Fig. 5b). Due to the higher v_{max} and lower E_{kp} the accumulated plastic strain, induced by dislocations gliding by kink-pair mechanism, reliefs the shear stress resulting in relatively long periods of viscous dislocation glide by kink-pair mechanism (Fig. 9a). The stress suffers more abrupt changes due to the interactions between carbon and dislocations (Fig. 9b). The experimentally observed average dislocation velocity at C=230 appm is 0.27 nm/s at $T = 200$°C [6]. The average dislocation velocity determined in the present simulations is 0.93 nm/s.

Formation of jogs resulting from kink collisions amount to self pinning points which reduce dislocation mobility. The present model does not take into account the effects of jog formation and self pinning on the dislocation mobility.

Preprints (www.preprints.org) | NOT PEER-REVIEWED | Posted: 24 March 2022 doi:10.20944/preprints202203.0319.v1

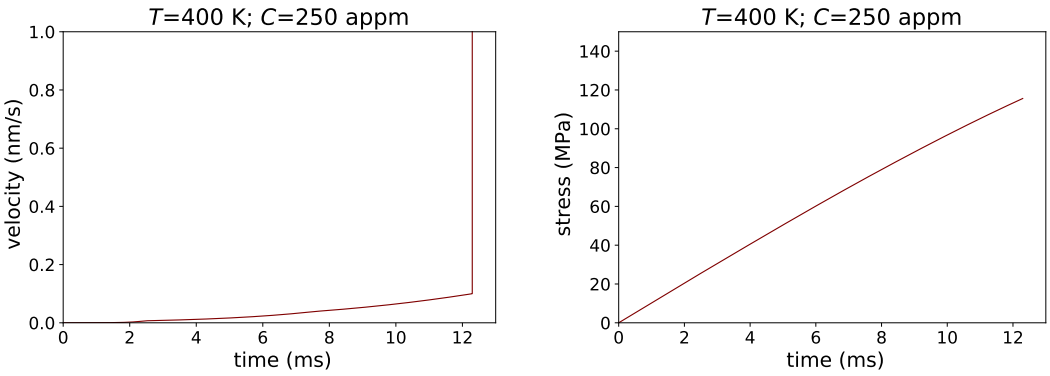

a) b)

Figure 8: Evolution of the dislocation velocity and stress with time during simulation of dislocation motion at T=400 K.

5 Conclusions

We have developed a self-consistent model for predicting velocity of 1/2[111] screw dislocation in binary iron–carbon alloys gliding by a high-temperature Peierls mechanism. The methodology of modelling includes:

- KMC simulation of carbon segregation in dislocation core and determination the total carbon occupancy of the core binding sites.
- Evaluation the effect of trapped carbon on motion of a straight dislocation segment between two adjacent Peierls valleys.
- Determination of kink-pair formation enthalpy E_{kp} of a screw dislocation in iron—carbon alloy.
- KMC simulation of carbon drag and determination of maximal dislocation velocity $v_{\max}$ at which the atmosphere of carbon atoms can follow a moving screw dislocation.
- Self consistent calculation of average velocity of screw dislocation in binary iron–carbon alloys gliding by a high-temperature kink-pair mechanism under constant strain rate.

We conduct a quantitative analysis of the conditions of stress and temperature at which screw dislocation glide is accomplished by a high-temperature kink-pair mechanism. We conclude that several factors are responsible for the viscous dislocatio glide observed above about 200°C in iron—carbon alloy:

Preprints (www.preprints.org) | NOT PEER-REVIEWED | Posted: 24 March 2022 doi:10.20944/preprints202203.0319.v1

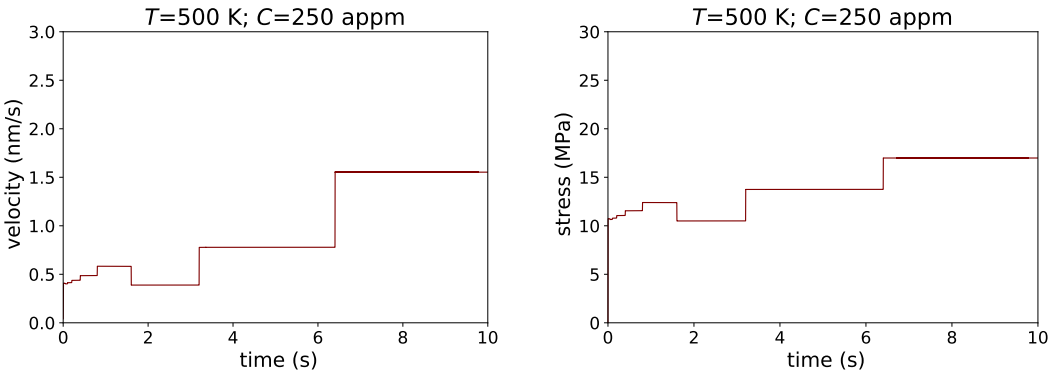

a) b)

Figure 9: Evolution of the dialocation velocity and stress with time during simulation of dislocation motion at T=500 K.

- At high temperatures kink-pair formation enthalpy E_{kp} decreases as a consequence of the increased carbon mobility in the dislocation core and reduced number of segregated C atoms.
- The enhanced diffusivity of carbon both in the core region and in dislocation surroundings lead to higher maximal dislocation velocity $v_{\max}$ at which the atmosphere of carbon atoms can follow a moving screw dislocation.

In accordance with the experimental observations the present simulations reveal that at high temperatures (T=500 K) 1/2[111] screw dislocation glide in iron–carbon alloy is accomplished by a high-temperature kink-pair mechanism. At intermediate temperatures (T=400 K) thermally-activated smooth dislocation propagation is interrupted by sporadic bursts controlled by athermal dislocation activity.

Acknowledgements

This research was supported in part by the Bulgarian Science Fund under the National Scientific Program “Petar Beron i NIE” (Project UMeLaMP), UKRI Grant EP/V001787/1 and by the European Regional Development Fund, within the Operational Programme “Science and Education for Smart Growth 2014–2020” under the Project CoE “National centre of mechatronics and clean technologies” BG05M20P001-1.001-0008-C01.

 doi:10.20944/preprints202203.0319.v1

References

[1] D. Caillard, An in situ study of hardening and softening of iron by carbon interstitials, Acta Mater. 59 (2011) 4974-4989.

[2] H. Fua, W. Song, E.I. Galindo-Nava, P.E.J. Rivera-Dáz-del-Castillo, Strain-induced martensite decay in bearing steels under rollingcontact fatigue: Modelling and atomic-scale characterisation, Acta Mater. 139 (2017) 163-173.

[3] A.H. Cottrell, B.A. Bilby, Dislocation theory of yielding and strain ageing of iron, Proc. Phys. Soc. Sect. A 62 (1949) 49-62.

[4] E. Clouet, S. Garruchet, H. Nguyen, M. Perez, C.S. Becquart, Dislocation interaction with C in α-Fe: A comparison between atomic simulations and elasticity theory, Acta Mater. 56 (2008) 3450-3460.

[5] Y. Li, P. Choi, C. Borchers, S. Westerkamp, S. Goto, D. Raabe, R. Kirchheim, Atomic-scale mechanisms of deformation-induced cementite decomposition in pearlite, Acta Mater. 59 (2011) 3965-3977.

[6] D. Caillard, Dynamic strain ageing in iron alloys: The shielding effect of carbon, Acta Mater. 112 (2016) 273-284

[7] I. H. Katzarov, L. B. Drenchev, D. L. Pashov, T. N. A. T. Zarrouk, O. Allahham, A. T. Paxton, Dynamic strain aging and the rôle Dynamic strain aging and the rôle of the Cottrell atmosphere, submitted for publication.

[8] Gh. Ali Nematollahi, Blazej Grabowski, Dierk Raabe, Joerg Neugebauer, Multiscale description of carbon-supersaturated ferrite in severely drawn pearlitic wires, Acta Materialia 111 (2016) 321-334.

[9] Peng Gong, Ivaylo H. Katzarov, John Nutter, Anthony T. Paxton and W. Mark Rainforth, The influence of hydrogen on plasticity in pure iron—theory and experiment, Scientific Reports 10 (2020) 10209.

[10] I. H. Katzarov, D. L. Pashov, and A. T. Paxton, Hydrogen embrittlement I. Analysis of hydrogen-enhanced localized plasticity: Effect of hydrogen on the velocity of screw dislocations in α-Fe. Phys. Rev. Mater. 1 (2017) 033602.

[11] Itakura, M. and Kaburaki, H. and Yamaguchi, M. and Okita, T., The Effect of Hydrogen Atoms on the Screw Dislocation Mobility in Bcc Iron: A First-Principles Study, Acta Materialia 61 (2013) 18.

[12] Clouet, E., Ventelon, L. Willaime, F. Dislocation core energies and core fields from first principles. Phys. Rev. Lett. 102, (2009), 055502.

[13] Paxton, A. T. and Elssser, C., Analysis of a Carbon Dimer Bound to a Vacancy in Iron Using Density Functional Theory and a Tight Binding Model, Phys. Rev. B 87 (2012) 22.

 doi:10.20944/preprints202203.0319.v1

[14] T. Zarrouk, Atomistic investigation of dislocation-assisted carbon migration in iron, PhD Theses, King's College London, 2022.

[15] Hirth, J. P. Lothe, J. Theory of Dislocations (McGraw-Hil Book Company, New York, (1968), 1 edn.

[16] Lisa Ventelon, B. Lüthi, E. Clouet, L. Proville, B. Legrand, D. Rodney, and F. Willaime, Dislocation core reconstruction induced by carbon segregation in bcc iron, Phys Rev B 91 (2015) 220102(R).

[17] G. Henkelman, and H. Jónsson, Improved tangent estimate in the nudged elastic band method for finding minimum energy paths and saddle points. J. Chem. Phys. 113 (2000) 9978–9985.

[18] M. Itakura, H. Kaburaki, and M. Yamaguchi. First-principles study on the mobility of screw dislocations in bcc iron. Acta Materialia, 60(9), (2012), 36983710.

[19] A. Y. Kuksin and A. V. Yanilkin, Atomistic simulation of the motion of dislocations in metals under phonon drag conditions, Phys. Solid State 55, (2013), 1010-1019.